Current Biology 22, 12–20, January 10, 2012 ©2012 Elsevier Ltd All rights reserved DOI 10.1016/j.cub.2011.11.028

Article

Genetic Dissection Reveals Two Separate Retinal Substrates for Polarization Vision in *Drosophila*

Mathias F. Wernet,[1] Mariel M. Velez,[1] Damon A. Clark,[1] Franziska Baumann-Klausener,[3] Julian R. Brown,[1,2] Martha Klovstad,[1] Thomas Labhart,[3] and Thomas R. Clandinin[1,*]

[1]Department of Neurobiology
[2]Howard Hughes Medical Institute
Stanford University, Stanford, CA 94305, USA
[3]Institute of Molecular Life Sciences, University of Zurich, 8057 Zurich, Switzerland

Summary

Background: Linearly polarized light originates from atmospheric scattering or surface reflections and is perceived by insects, spiders, cephalopods, crustaceans, and some vertebrates. Thus, the neural basis underlying how this fundamental quality of light is detected is of broad interest. Morphologically unique, polarization-sensitive ommatidia exist in the dorsal periphery of many insect retinas, forming the dorsal rim area (DRA). However, much less is known about the retinal substrates of behavioral responses to polarized reflections.

Summary: *Drosophila* exhibits polarotactic behavior, spontaneously aligning with the e-vector of linearly polarized light, when stimuli are presented either dorsally or ventrally. By combining behavioral experiments with genetic dissection and ultrastructural analyses, we show that distinct photoreceptors mediate the two behaviors: inner photoreceptors R7+R8 of DRA ommatidia are necessary and sufficient for dorsal polarotaxis, whereas ventral responses are mediated by combinations of outer and inner photoreceptors, both of which manifest previously unknown features that render them polarization sensitive.

Conclusions: *Drosophila* uses separate retinal pathways for the detection of linearly polarized light emanating from the sky or from shiny surfaces. This work establishes a behavioral paradigm that will enable genetic dissection of the circuits underlying polarization vision.

Introduction

Linearly polarized skylight created by atmospheric scattering of sunlight is perceived by many animals [1–3] and serves as an important navigational cue [4, 5]. Sunlight reflecting off shiny surfaces, such as leaves and water, is also linearly polarized [1, 6] and represents another environmental signal [7–9]. Behavioral, electrophysiological, and anatomical studies in many insects have identified specialized ommatidia in the dorsal rim area (DRA) of the compound eye as the most suitable candidate for detecting polarized skylight [10–12]. In these ommatidia, two photoreceptors maintain polarization sensitivity (PS) by failing to twist their rhabdomeres (for review, [12]). By comparison, much less is known about how insects detect polarized reflections. Behavioral studies in water bugs, dragonflies, locusts, and tabanid flies have demonstrated that polarized light can be detected by the ventral eye [7–9]. Although a likely retinal substrate has been described in the backswimmer *Notonecta* [6], the functional relationship between specific photoreceptors and these cues has not been demonstrated. Thus, understanding the cellular and behavioral relationship between dorsal and ventral polarization signals presents an important challenge.

The *Drosophila* eye comprises ~800 ommatidia, each containing eight photoreceptor cells, designated R1–R8. Outer photoreceptors, R1–R6, contain a blue/green-sensitive rhodopsin Rh1, associated with a UV-sensitizing pigment that confers response to UV light [13]. Variations in inner photoreceptors create a mosaic of at least three subtypes (see [14]). DRA ommatidia form a narrow band of 1–2 rows along the dorsal margin of the eye [15]. In these ommatidia, R7 and R8 have enlarged rhabdomeres and express the UV-sensitive pigment Rh3 [16, 17]. The two remaining subtypes are named "pale" (p) and "yellow" (y) and are randomly distributed across the retina [14]. R7 cells each express one of two UV opsins *rh3* (R7p), or *rh4* (R7y), whereas the underlying R8 cells express either *rh5* (R8p) or *rh6* (R8y). Due to this chromatic heterogeneity, inner photoreceptors are thought to mediate color vision [18–20].

Genetic tools provide powerful approaches to dissecting neural circuits underlying visual behaviors in *Drosophila* [19–22]. However, polarization vision is poorly understood in flies, because two previous studies implicated different retinal substrates. Von Philipsborn and Labhart [23] reported spontaneous turning responses of houseflies to slowly changing e-vector orientations, a behavior that was UV-specific and proposed to be mediated by DRA ommatidia. These findings agreed with electrophysiological and morphological studies demonstrating high PS in $R7_{DRA}$ and $R8_{DRA}$ photoreceptors [13, 24]. However, Wolf et al. [25] demonstrated alignment of *Drosophila* with the incident e-vector, a behavior that was elicited by both polarized UV and green light, even when presented ventrally, which they linked to R1–R6 photoreceptors. Here we establish a new behavioral paradigm and use genetic tools to define the retinal substrate of polarization vision in *Drosophila*.

Results

Drosophila Manifests Orientation Responses to Linearly Polarized Stimuli Presented Either Dorsally or Ventrally

Using a custom tracking system [22], we monitored the movements of isogenic fly populations in a circular arena (Ø 7.5 cm × height 2.5 cm) illuminated from above by linearly polarized (POL) light (Figure 1A; see also Figure S1 available online). Flies could freely walk on the transparent floor or ceiling of the arena, with either the dorsal or ventral eye seeing the stimulus. A polarizer, mounted on the motorized stage, rotated in 45° steps, remaining stopped for 5 s (Figure 1B). Flies were recorded from below using an infrared (IR) video camera, and the position and orientation of each fly were correlated with e-vector orientation during the stops. Polar histograms of fly angular headings during the stopped epochs suggested that flies preferentially aligned their body axis in

*Correspondence: trc@stanford.edu

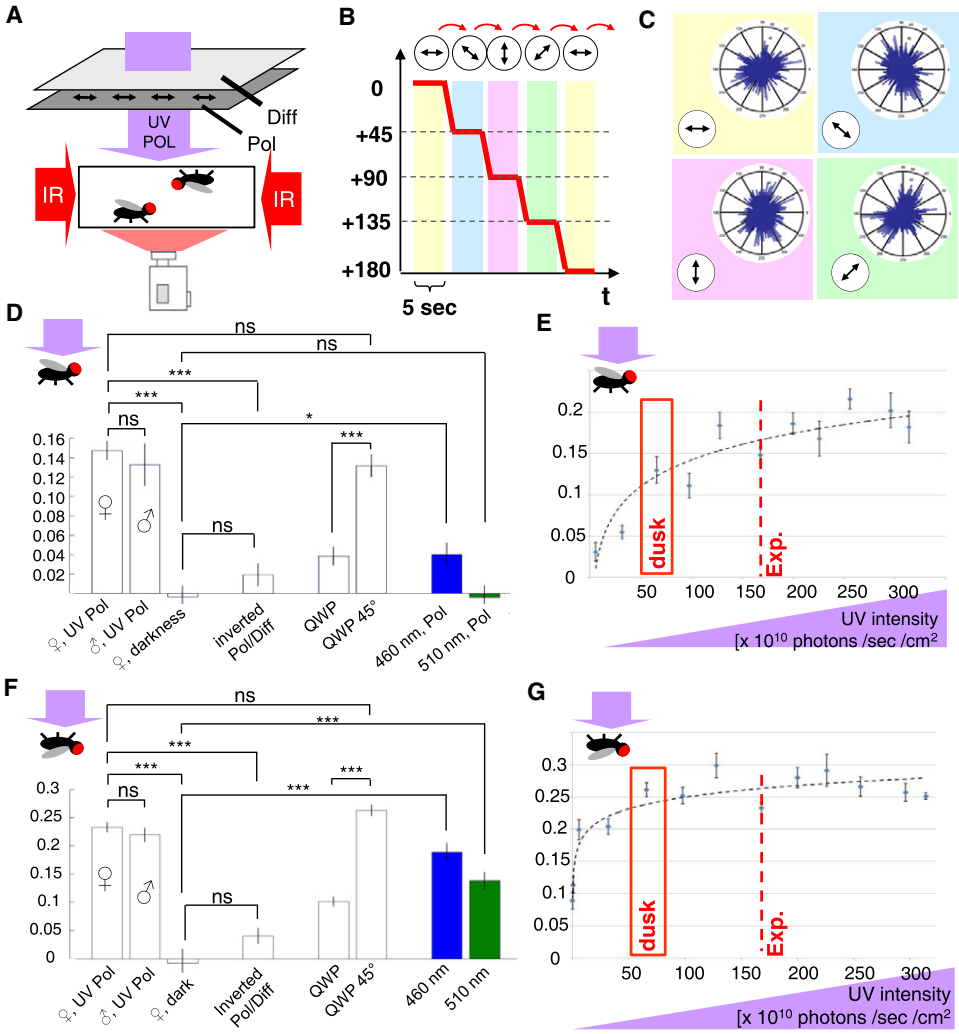

Figure 1. *Drosophila* Manifests Orientation Responses to Linearly Polarized Stimuli Presented Either Dorsally or Ventrally

(A) Schematic of the experimental setup used to present linearly polarized UV light from above to populations of *Drosophila*, which were filmed in the infrared from below. A polarization filter (HN42HE) was facing the flies, with two sheets of diffuser paper facing the light source. The following abbreviations are used: IR, infrared light; UV POL, polarized UV light; Diff, Diffuser; Pol, Polarizer.

(B) Summary of the stimulus protocol used. A computer-controlled servomotor rotated the polarization filter in 45° increments, remaining still for 5 s at each position. Different motor positions are denoted with different colors.

(C) Polar histograms of fly angular headings are shown for dorsally stimulated flies at each motor position.

(D) Basic description of wild-type polarotactic responses for linearly polarized UV stimulus presented dorsally. White bars symbolize UV-POL stimulation, green and blue bars symbolize stimulation with polarized light of the respective color (see Experimental Procedures). All error bars represent ±1 SEM; *p < 0.05, **p < 0.01, ***p < 0.001. The following abbreviation is used: ns, not significant.

(E) Alignment values A, plotted as a function of dorsal UV stimulus intensity. The dashed line represents intensity setting used for all subsequent experiments, and the red box represents UV intensity of skylight at dusk (Palo Alto, CA; see Supplemental Experimental Procedures).

(F) Basic description of wild-type responses for linearly polarized UV stimulus presented ventrally.

(G) A values plotted as a function of ventral UV stimulus intensity.

parallel with the e-vector (Figure 1C). Plotting these histograms on a linear axis over 360° revealed a sinusoidal modulation of orientation whose amplitude was proportional to the strength of the response and whose phase captured its precision. To represent this polarotactic behavior in a single metric, we computed an alignment value, A, incorporating both amplitude and phase of this distribution (see Experimental Procedures).

Both male and female flies aligned to the e-vector of a dorsal UV stimulus ($A_{♂}$ = 0.13 ± 0.02 and $A_{♀}$ = 0.15 ± 0.01; Figure 1D), across a range of ethologically relevant intensities (see Supplemental Experimental Procedures). This response was lost in complete darkness (A = 0.00 ± 0.01), or when the light was depolarized by a diffuser (A = 0.02 ± 0.01). Polarotactic responses were virtually lost (A = 0.04 ± 0.01) when a quarter wave plate (QWP) was positioned in front of the polarizer at an orientation that transformed the stimulus into circularly polarized light, which insects perceive as unpolarized (see Experimental Procedures, [26]). The responses could be restored by rotating the QWP 45° with respect to the polarizer, restoring linear polarization (A = 0.13 ± 0.01). Finally, dorsally stimulated flies did not orient to blue POL (460 ± 10 nm) or green POL (510 ± 10 nm) stimuli (A_{Blue} = 0.04 ± 0.01 and A_{Green} = 0.00 ± 0.01). Thus, the photoreceptors that mediate dorsal POL

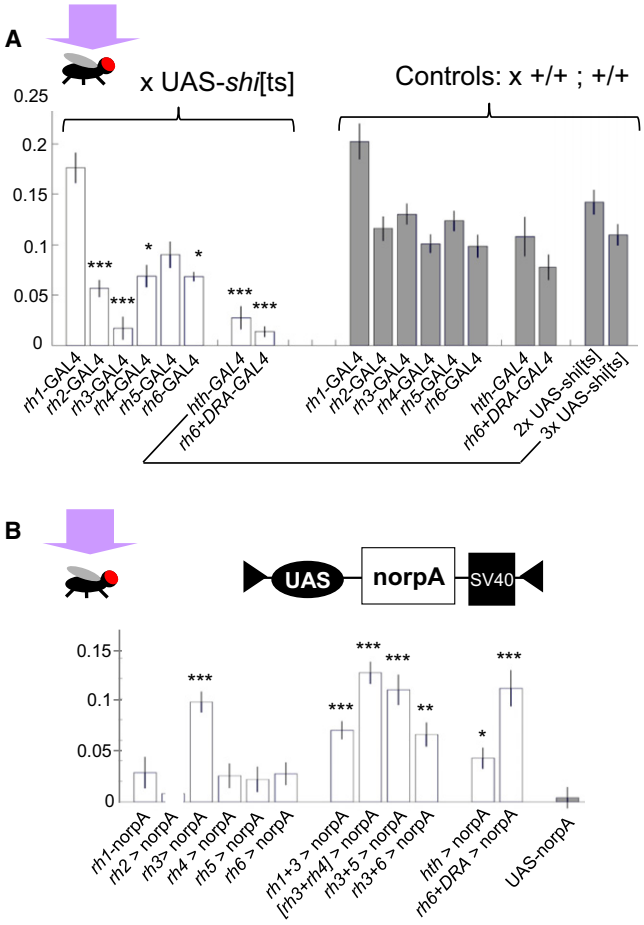

Figure 2. Dorsal Polarotactic Behavior Is Mediated by the Dorsal Rim Area

(A) Testing the necessity of photoreceptor subtypes mediating behavioral responses to UV-POL stimuli presented dorsally. Polarotactic responses were measured in flies expressing UAS-*shibire*^{ts} under the control of GAL4 drivers expressed in various subtypes of photoreceptors. Unlabeled bars were not significantly different from the control.

(B) Sufficiency of photoreceptor subtypes mediating behavioral responses to POL stimuli presented dorsally. Opsin drivers (both wild-type and mutated) and *hth*-GAL4 were used to rescue photoreceptor function by expressing eye-specific Phospholipase C (NorpA) from newly generated UAS-*norpA* transgenes (shown schematically, see Experimental Procedures), in *norpA*$^{-}$/ *norpA*$^{-}$ mutant flies. Open bars denote experimental genotypes, and gray bars denote negative controls (a *norpA*/*norpA* mutant, bearing *UAS-norpA*, without a GAL4 driver).

All error bars represent ± 1 SEM; *p < 0.05, **p < 0.01, ***p < 0.001.

behavior are strictly UV sensitive and detect the linearly polarized component of the stimulus.

In agreement with previous work demonstrating that *Drosophila* can perceive polarized light ventrally [25], both male and female flies displayed preferential alignment in parallel with the e-vector when seeing the polarized UV stimulus with the ventral half of their eyes (Figure 1F; A = 0.22 ± 0.01 and A = 0.23 ± 0.01, respectively), a response that was never detected in darkness (A = 0.01 ± 0.026). Ventral POL responses were significantly stronger than dorsal POL responses and remained robust down to low light levels (Figure 1G). Depolarizing the stimulus strongly abrogated the response (A = 0.04 ± 0.01) as did the QWP (A = 0.10 ± 0.01), and again the response could be rescued by rotating the QWP 45° (A = 0.26 ± 0.01). Robust ventral POL responses were also obtained using blue (460 nm) and green (510 nm) polarized light (A = 0.19 ± 0.02 and A = 0.14 ± 0.02, respectively), at the same intensities that failed to evoke responses when presented dorsally. Thus, the spectral sensitivity of ventral POL behavior is different, extending to longer wavelengths.

Dorsal Polarotactic Behavior Is Mediated by the Dorsal Rim Area

To determine the necessity of different photoreceptor classes for dorsal POL vision, we disrupted synaptic transmission through expression of *shibire*^{ts}, a temperature-sensitive, dominant-negative mutant of dynamin ([27]; Figure S2). Although expression in some photoreceptor subtypes nonspecifically reduced behavioral responses by less than 50% (Figure 2A), only inactivation using *rh3*-GAL4 (expressed in R7p and DRA inner photoreceptors) completely abolished polarotactic responses (A = 0.02 ± 0.01). Furthermore, dorsal POL behavior was completely lost upon photoreceptor inactivation using *hth*-GAL4 (expressed in $R7_{DRA}$ and $R8_{DRA}$; A = 0.03 ± 0.01), as well as *rh6*+DRA-GAL4 (A = 0.01 ± 0.005). In this driver, a point mutation introduced into the *rh6* promoter sequence leads to expression of GAL4 in R8y as well as $R7_{DRA}$ and $R8_{DRA}$ (Figure S2). Thus, DRA ommatidia provide the retinal substrate of dorsal POL vision. However, we could not rule out contributions of other photoreceptor classes.

To test for sufficient photoreceptor classes, we functionally rescued the phototransduction mutant *norpA* [28] using GAL4 drivers. As expected, *norpA* mutants were blind (A = 0.00 ± 0.001, Figure 2B). This defect was specifically rescued by expressing UAS-norpA using *rh3*-GAL4 (A = 0.10 ± 0.01) or *rh6*+DRA-GAL4 (A = 0.11 ± 0.02) but by none of the other opsin drivers. Rescue of different photoreceptor subclasses in addition to *rh3*-expressing cells (*rh1+rh3*, *rh3+rh4*, *rh3+rh5*, *rh3+rh6*) never led to A values significantly higher than *rh3* > norpA alone. Although *hth*-GAL4 did not rescue, this driver is only weakly expressed in the adult retina. Therefore, specifically restoring function to both $R7_{DRA}$ and $R8_{DRA}$ is sufficient to restore dorsal POL behavior.

The rhabdomeric photoreceptors of insects are inherently polarization sensitive because the rhodopsin molecules are aligned within the microvillar membrane so that linearly polarized light is maximally absorbed when the e-vector orientation is parallel to the microvilli [11, 29, 30]. Hence, polarization sensitivity is maximal when the microvilli are well aligned along the rhabomere [31, 32]. However, rhabdomeres are generally twisted in flies [33–36]. We therefore assessed rhabdomere twist of $R7_{DRA}$ and $R8_{DRA}$ (Figure 3) by measuring microvilli orientation in serial electron microscopic cross-sections. $R7_{DRA}$ and $R8_{DRA}$ were easily identifiable by their enlarged rhabdomeres (compare Figure 3A with Figure 3D; [15, 17]) and displayed strongly reduced twist when compared to non-DRA ommatidia (Figures 3A–3C and 3E). Based on the twist functions, we estimated their polarization sensitivity as $PS_{R7.DRA}$ = 8.1 ± 0.6 (n = 8) and $PS_{R8.DRA}$ = 7.9 ± 1.1 (n = 7) (see Supplemental Experimental Procedures). The e-vector orientations of maximal sensitivity (φ_{max}) of R7 and R8 were approximately orthogonal to each other (82° ± 8°). Thus, $R7_{DRA}$ and $R8_{DRA}$ have polarization sensitivity characteristics appropriate to an orthogonal analyzer system as previously described [2]. In contrast, R7 and R8 immediately adjacent to the DRA displayed considerable twisting (Figures 3B, 3C, and 3F), resulting in lower estimated PS

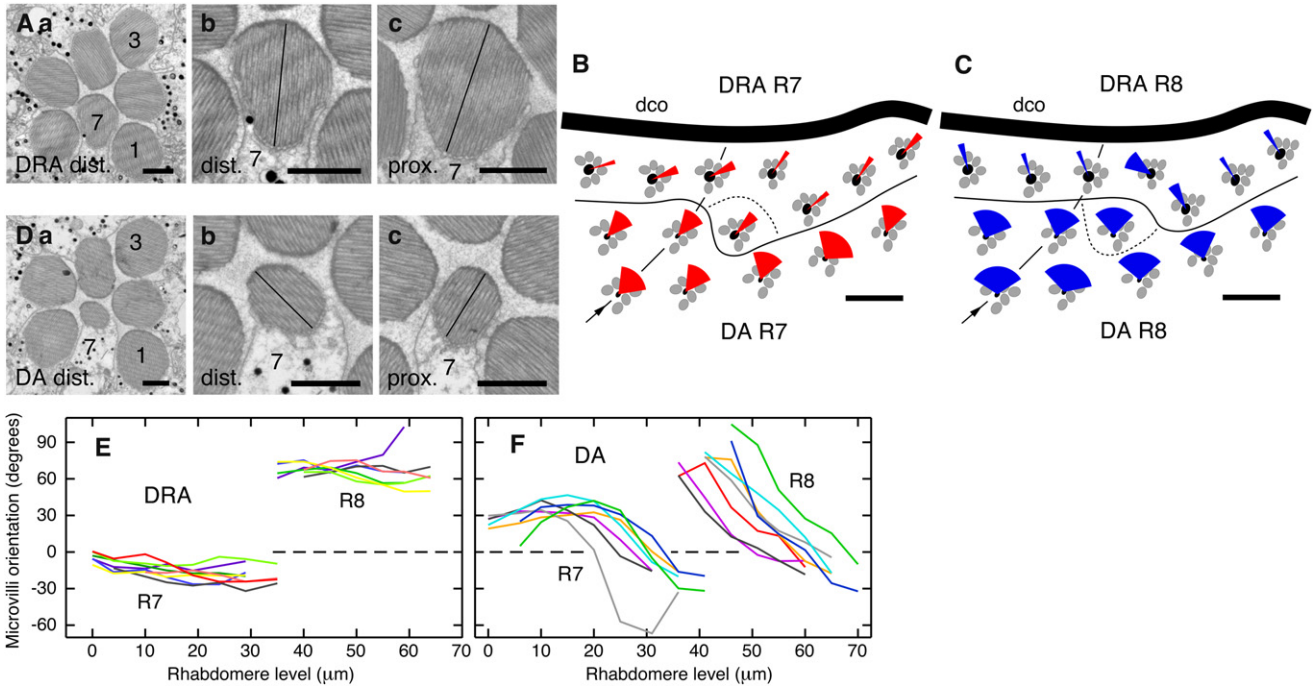

Figure 3. Rhabdomeres of Inner Photoreceptors in the Dorsal Rim Area Are Untwisted

Ommatidia of the dorsal rim area (DRA) and of the adjacent dorsal area (DA) were studied.

(A and D) Transmission electron micrographs showing rhabdom structure (a) and microvilli orientation of R7 in individual ommatidia at distal (b) and proximal (c) levels of R7. Numbers indicate receptor types. Straight lines in rhabdomere cross sections give microvilli orientations. Scale bars represent 1 μm.

(B and C) Total range of microvilli directions expressed by fans in different groups of ommatidia (same as in line graphs E and F). Red fans represent R7 and blue fans R8. A fine black line marks the boundary between the DRA and the DA. A fat black line shows the eye rim. Interrupted arrowed line is the v axis of the ommatidial pattern pointing dorsal (compare Figure S3D). The following abbreviation is used: dco, dorsocaudal origin of ommatidial rows. Scale bars represent 10 μm. Note that one ommatidium has a $R7_{DRA}$ (large, nontwisting rhabdomere) but a $R8_{DA}$ (small, twisting rhabdomere).

(E and F) Graphic representation of microvilli orientation at different retinal levels (twist functions) in R7 (left family of curves) and R8 (right family of curves). The ordinate indicates microvilli orientation relative to a straight line through the centers of R1 and R3 rhabdomeres (0°; stipled line). The abscissa gives retinal level relative to the surface of the eye (0 μm indicates level of first section containing rhabdoms). Colors mark data from different identified ommatidia.

values (PS_{R7} = 3.6 ± 1.2, n = 7; PS_{R8} = 2.2 ± 0.5, n = 8). R7 and R8 rhabdomeres at the ventral eye rim (VR) also exhibited significant twist and comparatively low estimated PS values ($PS_{R7.VR}$ = 2.6 ± 0.89, $PS_{R8.VR}$ = 2.2 ± 0.5, n = 5), consistent with the absence of a specialized ventral rim area.

Low Twist R7 Photoreceptors in the Ventral Eye Can Mediate Polarotactic Responses

We next assessed which photoreceptor classes are necessary for the ventral UV-POL response using *shibire^{ts}* (Figure 4A). Of the single opsin drivers, only *rh3*-GAL4 caused a significant response decrease (A = 0.11 ± 0.03). Inactivation of $R7_{DRA}$ and $R8_{DRA}$ using *hth*-GAL4 and *rh6*+DRA-GAL4 had no effect (A = 0.30 ± 0.01 and A = 0.29 ± 0.02, respectively). Thus, the DRA is not required for the ventral POL response. Rather, this behavior depends on UV-sensitive *rh3*-expressing ventral R7p cells.

Ventral POL responses to green light cannot be mediated by the exclusively UV-sensitive R7. In fact, inactivation of the three main photoreceptor classes by themselves (R1–R6, R7, or R8 cells) did not significantly affect the green-POL response (Figure 4B), which was only abrogated by a combination of *rh1*+(*rh5*+*rh6*)-GAL4 drivers (A = 0.02 ± 0.02). We infer that R1–R6 and R8, but not R7, are redundantly required for the response to green light (510 ± 10 nm). Hence, changing the stimulus wavelength shifted the retinal inputs to the POL vision circuitry.

To examine how the ventral retina mediates polarotactic responses, we estimated PS of ventral photoreceptors, by characterizing their rhabdomere twist (Figure 5). Because our behavioral data suggest a prominent role of R7p, we first compared rhabdomeric twist of R7 and R8 subtypes, after specifically labeling p ommatidia, using *rh3*-GAL4 and UAS-CD2:HRP (see Supplemental Experimental Procedures; Figures S3A and S3B). Specific differences in rhabdomeric twist between p and y ommatidia have been described for *Calliphora* R8 cells [33]. However, analysis of three patches of ventral retina revealed that R7p and R7y as well as R8p and R8y were equally twisted (Figure S3C). We next broadly searched the ventral retina, by analyzing rhabdomeric twist of R7 in seven, partly overlapping groups of 6 to 25 ventral ommatidia (Figure S3D). In four groups, R7 cells were significantly twisted, with an average estimated PS_{R7} ranging from 2.2 to 2.9 (Figure 5G; 2.2 ± 0.8, n = 11; 2.5 ± 0.6, n = 6; 2.9 ± 0.8, n = 11, 2.6 ± 0.9, n = 25). In two groups, twisting was restricted to the proximal half of the R7 rhabdomeres (Figure 5I) resulting in estimated PS of >3 in one group (PS_{R7} = 3.1 ± 0.4, n = 10), and reaching 5 in the other group (PS_{R7} = 5.0 ± 1.0, n = 7). The last group (Figures 5D, 5E, and 5H) contained several ommatidia with low twist (13° to 26°), resulting in high estimated PS values of 6.4 to 8.0 (average PS_{R7} of the group was 5.5 ± 1.6, n = 13). Comparison of R7 twist functions in three overlapping groups (VA2, VA5, VA6; Figure S3D) showed considerable differences between individuals, arguing against

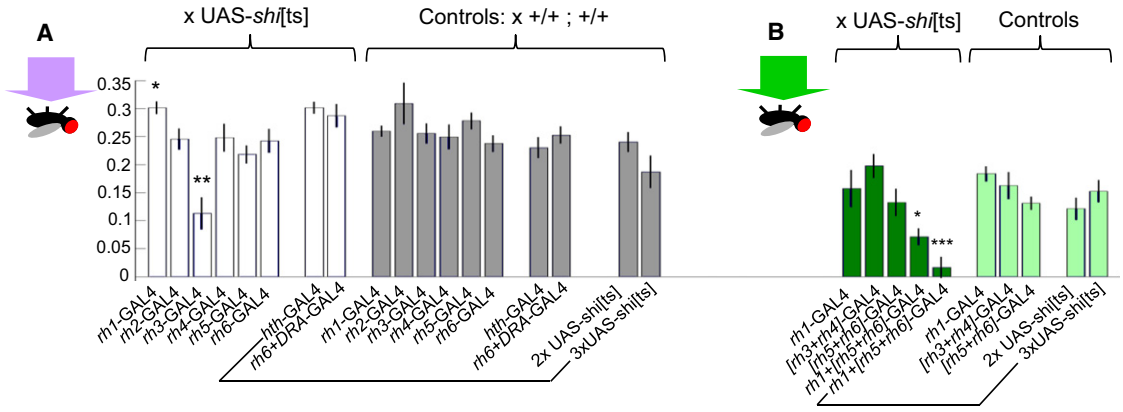

Figure 4. Ventral R7 Photoreceptors Can Mediate Polarotactic Responses

(A) Behavioral responses to a ventral POL stimulus after inactivation of photoreceptor subtypes with two copies of UAS-*shibire*^{ts}. Open bars denote experimental genotypes, and gray bars denote control genotypes.

(B) No single photoreceptor subtype is required for an orientation response of upside-down walking flies to linearly polarized green light, but behavior gets strongly abrogated upon simultaneous inactivation of *rh1*- and (*rh5*+*rh6*) subtypes and completely disappears using three copies of UAS-*shibire*^{ts} (compare dark and light green bars).

All error bars represent ± 1 SEM; *p < 0.05, **p < 0.01, ***p < 0.001.

a precisely defined ventral POL area. However, even in the more twisted rhabdomeres, the microvilli orientations still had a strong directional bias, resulting in significant PS. In addition, in each group, the φ_{max} orientations of R7 were strongly aligned, showing variations of only ±5.6° to ±13.6° (circular SD). Hence, by pooling the responses of neighboring ommatidia, even moderately polarization-sensitive R7 cells can provide reliable e-vector information.

The R8 cells in all ommatidial groups had strong rhabdomeric twist (Figures 5C and 5F–5I) and low estimated PS values with averages ranging from 1.5 to 2.2. Only in VA2, the group exhibiting strong estimated R7 PS (Figures 5F and 5H), a few R8 rhabdomeres were extremely short (10–20 μm), resulting in small net twist and correspondingly high estimated PS reaching 4–7 in five out of the 13 R8 cells.

Outer Photoreceptors R1–R6 Contribute to Ventral Polarotactic Responses

Using a ventral UV-POL stimulus, we assessed sufficiency of photoreceptor classes using UAS-norpA (Figure 6A). Only weak rescue was obtained when *norpA* was expressed in any of *rh1*-, *rh3*-, or *rh5*-positive cells (A = 0.09 ± 0.02, A = 0.07 ± 0.01, and A = 0.08 ± 0.02, respectively). However, *rh1*+*rh3* together rescued ventral POL responses to wild-type levels (A = 0.29 ± 0.02). Other combinations did not show this effect, and *hth*-GAL4 and *rh6*+DRA-GAL4 failed to rescue ventral POL behavior. Thus, specific synergy between R1–R6 and *rh3*-expressing R7p cells is required for a robust ventral UV POL response.

In contrast, under a green POL stimulus (Figure 6B), robust behavior was observed upon rescue of R1–R6 function (A = 0.24 ± 0.03). The QWP abrogated the behavioral response, both for wild-type, as well as *rh1*-norpA rescued animals, and rotation of the QWP by 45° again restored behavior. As expected, rescue of R7 cells, which cannot detect green light, was never sufficient (A = 0.00 ± 0.03). To our surprise, rescue of either R8 photoreceptor subtypes was sufficient to mediate ventral polarotaxis (A_{R8p} = A = 0.19 ± 0.01; A_{R8y} = 0.10 ± 0.01). Thus R1–R6 and R8 cells are sufficient to mediate responses to polarized green light presented ventrally.

To estimate PS of ventral R1–R6, we measured their twist functions (Figure 6C) in 17 ommatidia from three ventral groups. Whereas average estimated PS in R1–R3 was <2 (PS_{R1} = 1.7 ± 0.4, PS_{R2} = 1.7 ± 0.4, PS_{R3} = 1.8 ± 0.6, n = 17), PS in R4–R6 was enhanced (PS_{R4} = 3.0 ± 0.9, PS_{R5} = 2.8 ± 0.7, PS_{R6} = 2.4 ± 0.4, n = 17). Thus, ventral R4–R6 cells with their reduced twist can serve as an additional retinal substrate for ventral polarotaxis.

Discussion

We define the retinal substrates for both dorsal and ventral polarization vision in *Drosophila*. The DRA is necessary and sufficient for dorsal polarotactic responses, a result that strengthens studies in other insects, concluding that this region mediates responses to celestial polarized light [37–39]. In addition, our work defines the retinal substrate for responses to ventral polarotactic stimuli, as would occur naturally by reflections from shiny surfaces like water or leaves. Our work resolves the differences between previous behavioral studies of polarotactic behavior in flies [23, 25] by demonstrating that flies possess separate detectors to respond to distinct wavelengths, and sources, of polarized light.

A ventral POL region has previously been described in the backswimmer *Notonecta*, which uses polarized reflections to locate water bodies [6]. In this insect, inner photoreceptors in a small ventral region form orthogonal analyzer pairs with untwisted rhabdomeres much like a DRA [6]. *Drosophila* uses a different strategy by exploiting the fact that photoreceptors with moderate or weak twist still provide enough PS to serve as polarization analyzers. In this way, other visual senses, such as the detection of motion and spectral cues, should be affected only minimally by the polarization of light. Hence, unlike *Notonecta* with its specialized ventral retina, the generalist *Drosophila* incorporates ventral POL detectors while preserving other critical visual capacities.

An interesting feature of this design is that different classes of photoreceptors form ventral POL analyzers depending on stimulus wavelength. In the UV range, R7p cells are necessary for normal polarotactic responses; correspondingly, we describe ventral R7 cells with moderate to high estimated PS. However, our sufficiency experiments also revealed the

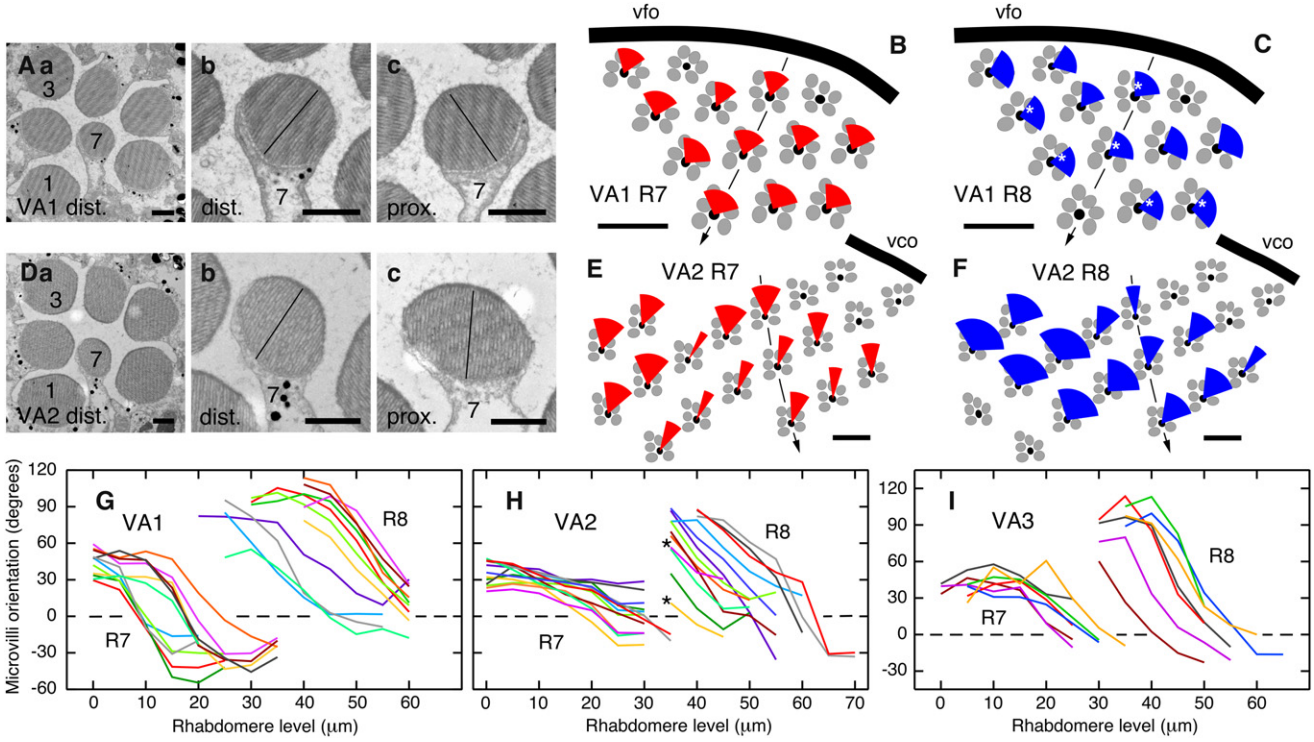

Figure 5. Moderate- and Low-Twist R7 Cells Exist in the Ventral Eye

Three different groups of ommatidia in the ventral eye (VA1, VA2, VA3). Rhabdomeres generally twist, but the amount of twist and the shape of the twist functions differed between groups.

(A and D) Same as in Figures 2A and 2D. Scale bars represent 1 μm.

(B, C, E, and F) Same as in Figures 2B and 2C (same ommatidia as in line graphs G and H). White asterisks on some fans in (C) indicate that data for the most proximal rhabdomere are missing. The following abbreviations are used: vfo, ventro-frontal; vco, ventro-caudal origin of ommatidial rows. Scale bars represent 10 μm.

(G–I) Same as in Figures 2E and 2F.

involvement of outer photoreceptors in polarization vision. Whereas R1–R3 appear to be weakly polarization sensitive, R4, R5, and possibly R6 show pronounced estimated PS due to reduced rhabdomeric twist. These results are consistent with intracellular recordings in *Calliphora* describing two classes of R1–R6, one of which retains some PS, even in the UV [40].

Whereas R4 to R6 with their pronounced PS provide a basis for ventral polarotaxis via the outer photoreceptors, the contribution of R8 is less clear. We found that R8 rhabdomeres twist strongly and, thus, R8 cells are expected to have low PS. In contrast, our behavioral tests demonstrate that R8 can rescue polarotaxis in norpA mutants (Figure 6B). Consistent with this, we found rare cases of very short R8 rhabdomeres exhibiting small twist ranges and correspondingly high expected PS. However, we cannot exclude the possibility that the apparent behavioral contributions of R8 could reflect low-level expression of our driver lines in R1–R6.

In larger flies, R7y and R8y as well as R1–R6 contain a UV-sensitizing pigment [13]. Because this molecule is not covalently linked to the opsin protein, its function is independent of microvillar orientation, thereby diminishing PS in the UV range [40]. In addition, these cells contain a C40 carotinoid, which both gives them their yellow appearance and induces anomalous dichroism, which further reduces PS [13]. This may explain why R7p, but not R7y, can mediate ventral UV polarotaxis in *Drosophila* (Figure 4). Our data describe an unexpected new role for "pale" ommatidia outside the DRA. Moreover, the behavioral data confirm that in R1–R6 the UV-sensitizing pigment does not completely eliminate PS in the UV, as was previously reported [40]. The contributions of the outer photoreceptors therefore become more pronounced when polarized green light is presented. That cellular contributions to ventral POL vision differ as a function of wavelength is particularly interesting because reflections from leaves contain much less UV (and more green light) than reflections from water [6]. Hence, activation of distinct combinations of photoreceptors might convey specific meanings to the fly.

The combination of polarization-sensitive outer and inner photoreceptors represents a new analyzer design, differing from those described in the DRA and the ventral retina of *Notonecta* [6]. In particular, our morphological data does not reveal an orthogonal organization of ventral analyzers. However, comparison between these channels might still increase quality and robustness of the signal. Nothing is known about the subtype-specific connectivity of R7p/R8p and their postsynaptic partners, and no electrophysiological data on polarization-opponent interneurons [41], or "compass neurons" [42], exist in flies. By establishing *Drosophila* as a model of polarization vision, our studies will enable genetic screens using quantitative behavioral assays to allow a complete dissection of the neural circuits involved in responding to this fundamental quality of light.

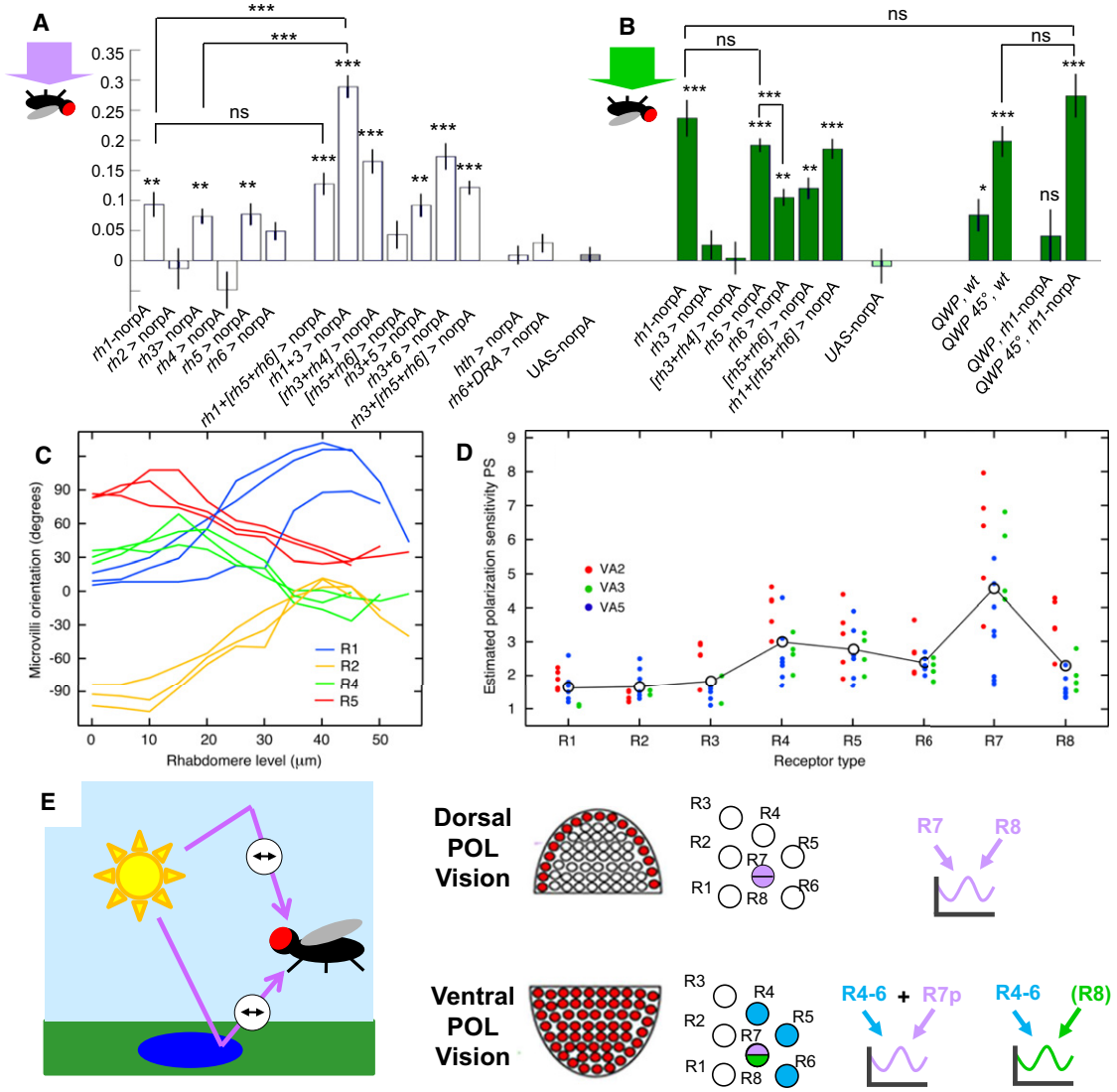

Figure 6. Outer Photoreceptors R1–R6 Contribute to Ventral Polarotaxis

(A) NorpA rescue experiments (open bars and shaded bar control) were used to define photoreceptor subtype sufficiency for behavioral responses to polarized UV light.

(B) Orienting responses to polarized green light in norpA rescue experiments. Alignment responses upon outer photoreceptors rescue (*rh1*-norpA) were eliminated by the quarter wave plate and restored by rotating it 45°.

(C) Twist functions of receptors R1, R2, R4, and R5. Typical twist functions of each cell type in three ommatidia are shown. The twist functions of R4 and R5 are generally flatter than those of R1 and R2.

(D) Polarization sensitivity (PS) of receptor types R1–R8. PS of samples of 4, 5, and 8 ommatidia in three different eyes are shown. Black circles indicate average PS. Note that R4, R5, and R6 have higher PS than R1–R3.

(E) Model summarizing photoreceptor contributions to linearly polarized stimuli presented to the dorsal or the ventral retina, respectively. Left panel shows that insects encounter linearly polarized light originating from atmospheric scattering or from reflections off of shiny surfaces such as water. Middle panel shows a schematic representation of the dorsal half (top) or ventral half (bottom) of the fly retina (necessary ommatidia are labeled red), followed by a schematic representation of photoreceptor classes in these ommatidia (photoreceptors that provide input to UV polarotaxis, green polarotaxis, or both behaviors are shown in violet, green, and blue, respectively). Right panel shows photoreceptor types providing behavioral contributions. Behavioral output is symbolized by a sinusoid function, and synergistic interactions between photoreceptor subtypes are symbolized by a "+" sign.

All error bars represent ± 1 SEM; *p < 0.05, **p < 0.01, ***p < 0.001. The following abbreviation is used: ns, not significant.

Experimental Procedures

Fly Stocks

The following fly stocks were provided: Oregon R, *norpA* [36], UAS-CD2:HRP on II, *rh3*-Gal4 on II, *rh4*-Gal4 on II, *rh5*-Gal4 on II, *rh6*-Gal4 on II (FlyBase, Indiana), UAS-*shibire*^{ts} on II and III (B. Baker, Stanford/Janelia Farm), *rh1*-Gal4 on X (J. Treisman, New York), *rh2*-Gal4 on II (A. Brand, Cambridge), *rh3+rh4-Gal4* on II, *rh5+rh6-Gal4* on II, *hth*-GAL4 (C. Desplan, New York), *rh1*-NorpA on III (R. Shortridge, Buffalo), UAS-CD8:GFP on X and II (C. Potter, Stanford/Baltimore), and *rh6*+DRA-GAL4 on II (T. Cook, Cincinnati).

Generation of UAS-norpA Transgenes

A ~900 bp 5′ fragment was PCR-amplifed from VDRC full-length complementary DNA clone GH28834 (primers: 5′-TGACGAATTCGGTACCGTG CAGGGCAACGGAAACGGAAGCGTC-3′, and 5′-CAACGTTTCTCCTCGTA GAGAGGGTA-3′). This product was cut with EcoRI/SacII and ligated into

pUAST (EcoRI/XhoI) together with a ~2.5 kb SacII/XhoI fragment excised from GH28834.

Immunohistochemistry

Brains were fixed for 45 min in 2% paraformaldehyde and blocked in 10% normal goat serum, then incubated with 1:10 mouse anti-24B10 (Developmental Studies Hybridoma Bank), 1:2,000 chicken anti-GFP (Abcam), and 10% normal goat serum and detected with goat-anti chicken Alexa 488 (Invitrogen) and goat anti-mouse Alexa 594 (Invitrogen) at a 1:200 dilution.

Behavior

All stocks were maintained on molasses, under 12:12 light/dark cycles, with circadian temperature changes between 18°C and 25°C, under 45%–60% humidity. Sixty-six mated female flies were collected 1–3 days after eclosion and sorted onto fresh food. After 2 days, flies were tested within 3 hr of the onset of light or 4 hr before the offset of light. All experiments were performed at 34°C.

Experimental Setup

An unpolarized light source (see below) illuminated a filter set consisting of a polarizer and a diffuser (polarizer/diffuser pair), which was rotated by a computer-controlled motor (software: NMC Simple Sequencer, Jeffrey Kerr). Within a large temperature-controlled (Peltier device) chamber, 66 flies were contained in a small arena formed by a heavily sanded plexiglass ring (Ø = 7.5 cm, height = 2.5 cm) between two plates of UV-transparent plexiglass. The distance from polarizer/diffuser pair was 3.5 cm for flies walking on the ceiling of the arena and 6 cm for those on the floor. The arena was surrounded by infrared LEDs (880 nm), and flies were filmed from below. Tracking software extracted the position and orientation of each individual fly in real time, at a rate of 30 Hz [22].

Stimulus

The light of an EXFO X-cite *exacte* DC light source passed one of three bandpass filter combinations. UV: Schott UV1 (365 ± 10 nm) + Thorlabs FGB37S, BLUE: Newport 20BPF10-460 (460 ± 10 nm) + FGL435S, or GREEN: Newport 20BPF10-510 (510 ± 10 nm) + FGL435S. All stimuli were calibrated with an Ocean Optics USB 2000 spectrophotometer. Polarizer (HN42HE, Polaroid) and diffuser (two sheets of tracing paper: "Transparentpapier," Max Bringmann KG, Germany) were illuminated through a 35 mm Zeiss collimating adaptor. The light stimulus was either linearly polarized or unpolarized depending on which side of the polarizer/diffuser pair faced the flies. The stimulus aperture was limited to 5 cm using a black plastic sheet with circular opening. Only flies walking directly under this aperture were tracked.

Metrics

A value: The alignment metric, A, for quantification of the behavioral response is extracted in several steps. (1) All fly angular headings during the stopped epochs for a given experiment are binned in 2° increments from 0 to 2π and transformed into a probability distribution. (2) This probability distribution was fitted to $A\times\cos(2\times\theta+\varphi)+b$ (where θ is the fly heading angle, φ the phase shift of the cosine function, and b is the offset). (3) A percent modulation (PM) = amplitude/mean (probability) was then calculated. (4) A value = PM × cos(φ). Thus, if the phase shift φ is zero, then the A value equals the PM. However, if φ is shifted, then the A value decreases. Inspection of the polar histograms revealed that the amplitude of the modulation (the strength of the behavioral response) was invariably coupled to the phase of the cosine function. That is, we never observed flies to align precisely at any position other than parallel to the e-vector.

Morphology

For electron microcopy (EM) of the dorsal-most retina, the eyes of wild-type *Drosophila* (Oregon R) were split in the horizontal plane. The dorsal eye halves were fixed with 2% glutaraldehyde in 0.05 M Na-cacodylate (pH 7.2) for 2 hr at 4°C and postfixed with 2% OsO_4 in 0.05 M Na-cacodylate (pH 7.2) for 2 hr at 4°C, followed by dehydration with 2,2 dimethoxypropane, and embedded in Epon 812. Silver sections were stained with uranyl acetate and lead citrate.

Tangential sections of groups of identified ommatidia were taken at 5 μm intervals and photographed in the electron microscope. Microvilli orientations were measured relative to a straight line through the rhabdomere centers of R1 and R3 as a reference. Twist functions were obtained by graphing microvilli orientation versus retinal level.

Supplemental Information

Supplemental Information includes three figures, Supplemental Results, and Supplemental Experimental Procedures and can be found with this article online at doi:10.1016/j.cub.2011.11.028.

Acknowledgments

The authors thank Bob Schneeveis, David Profitt, and Primoz Pirih for technical assistance. Claude Desplan, Bruce Baker, Russell Shortridge, Tiffany Cook, Jessica Treisman, and Martin Heisenberg provided fly stocks. This work was supported by the Helen Hay Whitney Foundation (M.F.W.), the Jane Coffin Childs Foundation (D.A.C.), the Stanford MSTP and a Ruth L. Kirschstein Graduate Fellowship Award (M.M.V.), and a National Institutes of Health Director's Pioneer Award (DP1 OD003530) (T.R.C.). This work was also supported by a Burroughs-Wellcome Career Development Award (T.R.C.), a Mcknight Scholar Award (T.R.C.), a Klingenstein Fellowship (T.R.C.), and a Searle Scholar Award (T.R.C).

Received: September 26, 2011
Revised: November 14, 2011
Accepted: November 15, 2011
Published online: December 15, 2011

References

1. Wehner, R. (2001). Polarization vision—a uniform sensory capacity? J. Exp. Biol. *204*, 2589–2596.
2. Wehner, R., and Labhart, T. (2006). Polarization vision. In Invertebrate Vision, E.J. Warrant and D.-E. Nilsson, eds. (Cambridge, UK: Cambridge University Press).
3. Nilsson, D.E., and Warrant, E.J. (1999). Visual discrimination: Seeing the third quality of light. Curr. Biol. *9*, R535–R537.
4. Rossel, S. (1993). Navigation by bees using polarized skylight. Comp. Biochem. Physiol. *104A*, 695–708.
5. Wehner, R. (2003). Desert ant navigation: how miniature brains solve complex tasks. J. Comp. Physiol. A Neuroethol. Sens. Neural Behav. Physiol. *189*, 579–588.
6. Schwind, R. (1983). Zonation of the optical environment and zonation in the rhabdom structure within the eye of the backswimmer, Notonecta glauca. Cell Tissue Res. *232*, 53–63.
7. Wildermuth, H. (1998). Dragonflies recognize the water of rendezvous and oviposition sites by horizontally polarized light: a behavioral field test. Naturwissenschaften *85*, 297–302.
8. Shashar, N., Sabbah, S., and Aharoni, N. (2005). Migrating locusts can detect polarized reflections to avoid flying over the sea. Biol. Lett. *1*, 472–475.
9. Horváth, G., Majer, J., Horváth, L., Szivák, I., and Kriska, G. (2008). Ventral polarization vision in tabanids: horseflies and deerflies (Diptera: Tabanidae) are attracted to horizontally polarized light. Naturwissenschaften *95*, 1093–1100.
10. Labhart, T., and Meyer, E.P. (2002). Neural mechanisms in insect navigation: polarization compass and odometer. Curr. Opin. Neurobiol. *12*, 707–714.
11. Hardie, R.C. (1984). Properties of photoreceptors R7 and R8 in dorsal marginal ommatidia in the compound eyes of *Musca* and *Calliphora*. J. Comp. Physiol. A Neuroethol. Sens. Neural Behav. Physiol. *154*, 157–165.
12. Labhart, T., and Meyer, E.P. (1999). Detectors for polarized skylight in insects: a survey of ommatidial specializations in the dorsal rim area of the compound eye. Microsc. Res. Tech. *47*, 368–379.
13. Hardie, R.C. (1985). Functional organization of the fly retina. In Progress in Sensory Physiology, H. Autrum, D. Ottoson, E.R. Perl, R.F. Schmidt, H. Shimazu, and W.D. Willis, eds. (Berlin: Springer), pp. 1–79.
14. Wernet, M.F., and Desplan, C. (2004). Building a retinal mosaic: cell-fate decision in the fly eye. Trends Cell Biol. *14*, 576–584.
15. Wada, S. (1974). Spezielle randzonale Ommatidien der Fliegen (Diptera: Brachycera): Architektur und Verteilung in den Komplexaugen. Z. Morph. Tiere *77*, 87–125.
16. Fortini, M.E., and Rubin, G.M. (1991). The optic lobe projection pattern of polarization-sensitive photoreceptor cells in *Drosophila melanogaster*. Cell Tissue Res. *265*, 185–191.

17. Wernet, M.F., Labhart, T., Baumann, F., Mazzoni, E.O., Pichaud, F., and Desplan, C. (2003). Homothorax switches function of *Drosophila* photoreceptors from color to polarized light sensors. Cell *115*, 267–279.
18. Heisenberg, M., and Buchner, E. (1977). The role of retinula cell types in visual behavior of *Drosophila melanogaster*. J. Comp. Physiol. *117*, 127–162.
19. Gao, S., Takemura, S.Y., Ting, C.Y., Huang, S., Lu, Z., Luan, H., Rister, J., Thum, A.S., Yang, M., Hong, S.T., et al. (2008). The neural substrate of spectral preference in *Drosophila*. Neuron *60*, 328–342.
20. Yamaguchi, S., Desplan, C., and Heisenberg, M. (2010). Contribution of photoreceptor subtypes to spectral wavelength preference in *Drosophila*. Proc. Natl. Acad. Sci. USA *107*, 5634–5639.
21. Rister, J., Pauls, D., Schnell, B., Ting, C.Y., Lee, C.H., Sinakevitch, I., Morante, J., Strausfeld, N.J., Ito, K., and Heisenberg, M. (2007). Dissection of the peripheral motion channel in the visual system of *Drosophila melanogaster*. Neuron *56*, 155–170.
22. Katsov, A.Y., and Clandinin, T.R. (2008). Motion processing streams in Drosophila are behaviorally specialized. Neuron *59*, 322–335.
23. von Philipsborn, A., and Labhart, T. (1990). A behavioural study of polarization vision in the fly, *Musca domestica*. J. Comp. Physiol. A Neuroethol. Sens. Neural Behav. Physiol. *167*, 737–743.
24. Wunderer, H., and Smola, U. (1982a). Fine structure of ommatidia at the dorsal eye margin of *Calliphora Erythrocephala Meigen* (Diptera: Calliphoridae): an eye region specialized for the detection of polarized light. Int. J. Insect Morphol. Embryol. *11*, 25–38.
25. Wolf, R., Gebhardt, B., Gademann, R., and Heisenberg, M. (1980). Polarization sensitivity of course control in *Drosophila melanogaster*. J. Comp. Physiol. *139*, 177–191.
26. Labhart, T. (1996). How polarization-sensitive interneurones of crickets perform at low degrees of polarization. J. Exp. Biol. *199*, 1467–1475.
27. Kitamoto, T. (2001). Conditional modification of behavior in *Drosophila* by targeted expression of a temperature-sensitive shibire allele in defined neurons. J. Neurobiol. *47*, 81–92.
28. Bloomquist, B.T., Shortridge, R.D., Schneuwly, S., Perdew, M., Montell, C., Steller, H., Rubin, G.M., and Pak, W.L. (1988). Isolation of a putative phospholipase C gene of *Drosophila*, norpA, and its role in phototransduction. Cell *54*, 723–733.
29. Israelachvili, J.N., and Wilson, M. (1976). Absorption characteristics of oriented photopigments in microvilli. Biol. Cybern. *21*, 9–15.
30. Goldsmith, T.H., and Wehner, R. (1977). Restrictions on rotational and translational diffusion of pigment in the membranes of a rhabdomeric photoreceptor. J. Gen. Physiol. *70*, 453–490.
31. Wehner, R., Bernard, G.D., and Geiger, E. (1975). Twisted and non-twisted rhabdoms and their significance for polarization detection in the bee. J. Comp. Physiol. *104*, 225–245.
32. Nilsson, D., Labhart, T., and Meyer, E.P. (1987). Photoreceptor design and optical properties affecting polarization sensitivity in ants and crickets. J. Comp. Physiol. A Neuroethol. Sens. Neural Behav. Physiol. *161*, 645–658.
33. Wunderer, H., and Smola, U. (1982b). Morphological differentiation of the central visual cells R7/8 in various regions of the blowfly eye. Tissue Cell *14*, 341–358.
34. Smola, U., and Tscharntke, H. (1979). Twisted rhabdomeres in the Dipteran eye. J. Comp. Physiol. *133*, 291–297.
35. Smola, U., and Wunderer, H. (1981a). Fly rhabdomeres twist in vivo. J. Comp. Physiol. *142*, 43–49.
36. Smola, U., and Wunderer, H. (1981b). Twisting of blowfly (*Calliohora erythrocephala Meigen*) (Diptera, Calliphoridae) rhabdomeres: an in vivo feature unaffected by prepreation or fixation. Int. J. Insect Morphol. Embryol. *10*, 331–344.
37. Stalleicken, J., Labhart, T., and Mouritsen, H. (2006). Physiological characterization of the compound eye in monarch butterflies with focus on the dorsal rim area. J. Comp. Physiol. A Neuroethol. Sens. Neural Behav. Physiol. *192*, 321–331.
38. Brunner, D., and Labhart, T. (1987). Behavioural evidence for polarization vision in crickets. Physiol. Entomol. *12*, 1–10.
39. Mappes, M., and Homberg, U. (2004). Behavioral analysis of polarization vision in tethered flying locusts. J. Comp. Physiol. A Neuroethol. Sens. Neural Behav. Physiol. *190*, 61–68.
40. Guo, A. (1981). Elektrophysiologische Untersuchungen zur Spektral- und Polarisationsempfindlichkeit der Sehzellen von *Calliphora erythrocephala* III. Sci. Sin. *24*, 272–286.
41. Labhart, T. (1988). Polarization-opponent interneurons in the insect visual system. Nature *331*, 435–437.
42. Heinze, S., and Homberg, U. (2007). Maplike representation of celestial E-vector orientations in the brain of an insect. Science *315*, 995–997.